Available online at www.sciencedirect.com
SCIENCE DIRECT
Polymer 46 (2005) 8573–8581
polymer
www.elsevier.com/locate/polymer

Polymer-layered silicate nanocomposites prepared through in situ reversible addition–fragmentation chain transfer (RAFT) polymerization

Nuha Salem, Devon A. Shipp*

Department of Chemistry and Center for Advanced Materials Processing, Clarkson University, Potsdam, NY 13699-5180, USA

Received 31 January 2005; accepted 14 April 2005
Available online 13 June 2005

Abstract

Reversible addition–fragmentation chain transfer (RAFT) polymerizations were performed in the presence of organically modified clays and successfully prepared polystyrene-, poly(methyl methacrylate)-, and poly(*n*-butyl acrylate)-layered silicate nanocomposites. The polymers had well-defined molecular weights and low polydispersities, as expected from RAFT polymerizations. The morphology of polystyrene-, and poly(*n*-butyl acrylate)-nanocomposites were found to be exfoliated using montmorillonite modified with *N*,*N*-dimethyl-*n*-hexadecyl-(4-vinylbenzyl) ammonium (MMT-VB16). In the case of PMMA nanocomposite, the structure was a mixture of intercalated and exfoliated when MMT-VB16 was used, while the use of montmorillonite modified with 2-methacryloyloxyethyl-hexadecyldimethyl ammonium (MMT-MA16) resulted in exfoliation.

Keywords: Reversible addition–fragmentation chain transfer; Chain transfer agents; X-ray diffraction

1. Introduction

Polymer-layered silicate nanocomposites (PLSNs) have recently gained popularity because of improvements in various material properties without deleterious consequences [1–11]. Such properties include increases in modulus, strength, heat resistance, and reductions in gas permeability and flammability [12,13]. For example, it has been found that performing polymerizations in the presence of organically modified silicates may lead to significant dispersion of the nanometer thick silicate layers in the polymer matrix. It was found that the presence of 5% wt/wt silicate in nylon-6-layered silicate nanocomposite shows substantial improvements in various physical properties over those for the pure nylon-6. For example, the nanocomposite showed an improvement of 40% in the tensile strength, 68% in tensile modulus, 60% in flexural strength, and 126% in flexural modulus. The heat distortion temperature (HDT) is also increased from 65 to 152 °C [13].

We, and others, have recently shown that PLSNs, with well-dispersed (exfoliated) silicate layers, can be produced using the living radical polymerization (LRP) methods of atom transfer radical polymerization (ATRP) [14–17] and nitroxide-mediated polymerization (NMP) [18,19]. LRPs [20–31] have proven to be successful in the preparation of well-defined polymers in bulk, solution, suspension, and in microemulsion polymerizations, and utilizing these methods allows for the examination of several aspects of PLSNs such as morphology dependence on molecular weight, mode and degree of polymer chain tethering to the silicate layers, and the production of novel PLSN materials such as block copolymers [16]. However, the main drawback of ATRP is that the final product is contaminated with a metal catalyst residue (often copper salts). In order to expand the repertoire of vinyl monomers that can be polymerized in situ to form PLSNs we have turned our attention to reversible addition–fragmentation chain transfer (RAFT) polymerization [31]. RAFT does not rely on a metal catalyst and can polymerize a wide range of monomers, theoretically all those monomers that can polymerize via a radical intermediate. The reason for the versatility of the RAFT process is its tolerance to the reaction conditions such as solvent and temperature [31]. It can be used to make a number of polymer architectures (e.g. star, graft, microgel polymers) and compositions (e.g. statistical, gradient and

* Corresponding author. Tel.: +1 315 268 2393; fax: +1 315 268 6610.
E-mail address: dshipp@clarkson.edu (D.A. Shipp).

0032-3861/$ - see front matter © 2005 Elsevier Ltd. All rights reserved.
doi:10.1016/j.polymer.2005.04.082

block copolymers). We are interested in making such complex, yet well-defined, polymers in the presence of silicates not only to develop new materials but also to provide a basic understanding of morphology development and structure-property relationships. To this end we wish to initially develop basic conditions in which control over molecular weights can be achieved through LRP in the presence of layered silicates that preferably yield well-exfoliated nanocomposites.

In this paper we report the preparations of PS-, PBA- and PMMA-montmorillonite nanocomposites that have well-controlled molecular weights and narrow polydispersities using RAFT polymerization in bulk. This represents the first reported synthesis of such nanocomposites using RAFT polymerization. We show that exfoliated nanocomposite structures can be obtained with polymers that are molecularly well-defined. Techniques such as GPC, XRD, TGA, and TEM have been used to study progress of the polymerizations and the morphology of the nanocomposites.

2. Experimental

2.1. Materials

Styrene (Fisher), *n*-butyl acrylate (BA) and methyl methacrylate (MMA) (Aldrich), were distilled under reduced pressure and purged with N_2 gas before use. *N*,*N*-Dimethyl-*n*-hexadecyl-(4-vinylbenzyl) ammonium chloride (VB16) and 2-methacryloyloxyethyl-hexadecyldimethyl ammonium bromide (MA16) were prepared and used to modify the montmorillonite (MMT) according to literature procedures [5,11] to give the organically modified MMTs MMT-VB16 and MMT-MA16, respectively. MMT was kindly supplied by southern clay products (ion-exchange capacity = 92 mequiv./100 g). Azoisobutryronitrile (AIBN; Kodak) was recrystallized from methanol. The chain transfer agents (CTAs) used were 4-cyano-4-methyl-4-thiobenzoylsulfanylbutyric acid (CTA-1) and 2-(2-cyano-propyl) dithiobenzoate (CTA-2), which were prepared according to McCormick et al. [32] and Thang et al. [33], respectively.

2.2. Preparation of N,N-dimethyl-n-hexadecyl-(4-vinylbenzyl) ammonium chloride (VB16) and 2-methacryloyloxyethyl-hexadecyldimethyl ammonium bromide (MA16)

VB16 was prepared according to Wilkie et al. [15] by mixing 5.5 ml (0.0465 mol) of 4-vinylbenzyl chloride and 17.7 ml (0.05 mol) of *N*,*N*-dimethyl-*n*-hexadecylamine in 53 ml ethyl acetate and the solution was stirred at 40 °C overnight. The reaction mixture was then filtered and the white precipitate of *N*,*N*-dimethyl-*n*-hexadecyl-(4-vinyl-benzyl) ammonium chloride (VB16) was recrystallized from ethyl acetate. After drying in a vacuum oven at room temperature, the resulting VB16 was analyzed using ^{1}H NMR. MA16 was prepared according to Zeng and Lee [5] by reacting 2-dimethylamino ethyl methacrylate with 1-bromohexadecane (2:1 molar ratio, respectively) in the presence of the inhibitor hydroquinone monomethyl ether (1000 ppm) at 60 °C for 24 h using ethyl acetate as a solvent. The resulting precipitate of 2-methacryloyloxyethyl-hexadecyldimethyl-ammonium bromide (MA16) was filtered, dried in a vacuum oven and then analyzed by ^{1}H NMR.

2.3. Modification of MMT using VB16 and MA16

25 g of MMT was dispersed in 1 l distilled water by stirring overnight. 11.52 g of VB16 (30 mmol) was dissolved in 100 ml distilled water then added drop wise to the dispersed clay in water with continuous stirring at 0–5 °C. The stirring was continued for more 3 h at 0–5 °C before the MMT-VB16 was filtered and washed several times with distilled water until a negative test for the presence of the chloride ion in the filtrate was achieved. The VB16 modified MMT was dried in the vacuum oven at room temperature followed by stirring in petroleum ether for 1 h, filtration and washing with petroleum ether several times. The MMT-VB16 was dried in the vacuum oven until constant weight was obtained and then characterized for the presence of the organic modifier in the interlayer space by XRD and TGA. MMT-MA16 was prepared using the same procedure and replacing the 30 mmol of VB16 with 30 mmol of MA16.

2.4. Preparation of polymer-silicate nanocomposites

PS, PBA, and PMMA clay nanocomposites were prepared in bulk using RAFT polymerization in the presence of organically modified MMT. An example is the RAFT polymerization of styrene: 0.232 g CTA-2 (1.05 mmol), 1.0 g MMT-VB16, and 0.0517 g AIBN (0.315 mmol), were dissolved in 36.0 ml styrene (315 mmol) in a Schlenk flask under N_2 gas atmosphere. The mixture was stirred until homogeneous dispersion was obtained. The molar ratio of the styrene:CTA-2:AIBN was 300:1:0.3, respectively, and the weight % of MMT-VB16:monomer = 3%. The polymerization was performed in oil bath at 110 °C. The same procedure was followed for MMA and BA at 60 °C using CTA-1. Samples were taken via a degassed syringe at various time intervals for the kinetic studies. The molar ratio of the monomer to the RAFT agent was chosen to be 300:1 to get the targeted molecular weight of 30,000 g/mol assuming that every mole of RAFT agent will initiate one chain of the polymer.

2.5. Measurements

Monomer conversions were measured gravimetrically. A gel permeation chromatograph (GPC) equipped with a

Waters 717 autosampler, a Waters 515 HPLC pump, and a Viscotek LR40 refractometer, with THF as an eluent was used to measure the molecular weight and the molecular weight distribution of the polymers. PS standards were used for PS and PBA measurements, while PMMA standards were used for the PMMA samples. For the GPC measurements, polymers were detached from the clay through refluxing for about 3 h in THF/LiBr solution (5 wt%), followed by centrifugation and filtration through 0.2-μm filters. Transmission electron microscopy (TEM) was carried out on a JEOL JEM-1200EX electron microscope operated at 120 kV and the samples were sliced using ultramicrotome with a glass knife. Thermogravemetric analysis (TGA) was performed on a Perkin–Elmer TGA 7 operating under air. X-ray diffraction (XRD) spectra were collected on a Siemens D5000 diffractometer equipped with an intrinsic germanium detector system with Cu K_α radiation ($\lambda = 1.5406$ Å).

3. Results and discussion

MMT was modified with VB16 (MMT-VB16) and MA16 (MMT-MA16) via a solution intercalation procedure. TGA data obtained for the original MMT, MMT-VB16 and MMT-MA16 are shown in Fig. 1. From this data it is observed that VB16-MMT is more thermally stable than MA16-MMT presumably because of the presence of the phenyl ring in the VB16 that imparts greater stability compared to the ester group in MA16 that may undergo decomposition at lower temperatures. From the TGA data, the calculated organic content for MMT-VB16 is 27.13 wt% while for MMT-MA16 it is 30.0 wt%. These data represent almost 100% exchange of the Na^+ with the ammonium cations for both VB16 and MA16. XRD analysis (Fig. 2) shows that spacing between the silicates layers have been

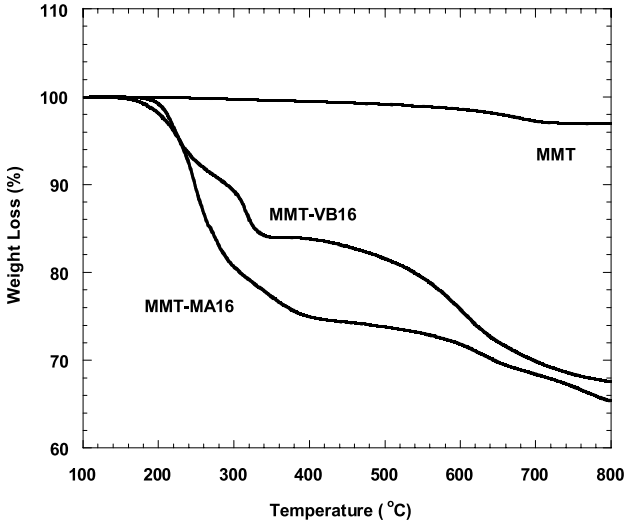

Fig. 1. TGA thermograms of unmodified MMT, MMT-VB16, and MMT-MA16.

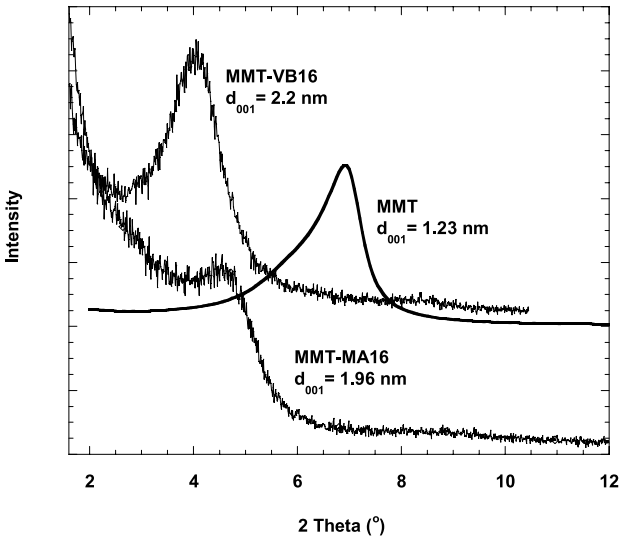

Fig. 2. XRD patterns of MMT, MMT-VB16, and MMT-MA16.

increased by 0.97 and 0.73 nm after modification with VB16 and MA16, respectively, which is an evidence of the successful intercalation of both modifiers in the MMT layers.

RAFT polymerization of styrene, BA, and MMA initiated by AIBN in the presence of MMT-VB16 was carried out (Scheme 1). Styrene polymerization was mediated using CTA-2, while BA and MMA were mediated by CTA-1. No difference in reactivity or morphology was expected by the presence of the carboxyl group in CTA-1 compared with CTA-2. Samples taken at various time intervals and analyzed for monomer conversion and molecular weight clearly indicate that the RAFT polymerizations were successful in terms of controlling the molecular weight and the molecular weight distribution (Figs. 3–5). The polydispersities, M_w/M_n, of all samples taken during the kinetic study were ≤ 1.5 which indicates a narrow molecular weight distribution in the polymer sample. Figs. 3–5 show the evolution of the molecular weight and polydispersities with monomer conversion for each of the three polymer nanocomposites. Linear evolution of PS molecular weight with monomer conversion was observed (Fig. 3); the actual and expected molecular weights are in good agreement. GPC data was obtained for both tethered and free polymer for the final sample of PS and the molecular weight was found to be the same ($M_n =$ 26,000, $M_w/M_n = 1.18$) in both cases. Thus we conclude that free polymer chains and tethered polymer chains grow under the same conditions. We also determined that 20 wt% of the polymer chains were attached to the silicate layers. This corresponds to 28% of the ion exchange capacity of the VB16 modified MMT. Since 100% exchange was noted in the MMT-VB16, this difference may indicate that some of the VB16 moieties may not become involved in the polymerization. However, in this exfoliated system (see below) with such a percentage of chains attached to the

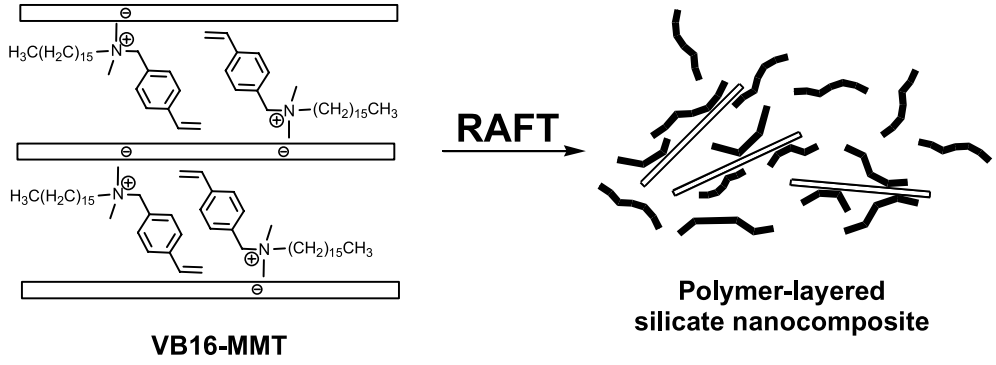

Scheme 1.

silicate layers (20 wt%) and with both chain populations being identical in molecular weight and polydispersity we can conclude that some of the VB16 moieties are accessible for polymerization and no difference in mechanism is discernable.

For the BA polymerization the molecular weight evolution vs. % conversion (Fig. 4) shows a good match between expected and actual molecular weights and the polydispersities are low, providing evidence of the efficiency of using RAFT polymerization to control the polymerization of BA. However, the polymerization kinetic data of PBA (Fig. 6) show an induction period of about 2–3 h before the polymerization occurred, and a limiting conversion of approximately 60% after 36–48 h. Such results have been previously observed during the RAFT polymerization of acrylates on a regular basis, and while the cause has been debated [34–39] it seems this is due to differences in addition rates of the initiating radical (derived from the CTA) to monomer compared with the addition rates of the propagating radical to monomer [40–42].

Data obtained for PMMA (Fig. 5) also indicate that excellent control over the polymerization was achieved up to high conversion (99% monomer conversion). There was no apparent induction period during the MMA polymerization (Fig. 6). PMMA-MMT-VB16 was also prepared using CTA-2 in order to determine if there is any difference between CTA-1 and CTA-2 in term of controlling the polymerization. As shown in Fig. 5, there seems to be no differences between the two CTAs used in terms of molecular weight development. It was found that only ~3% of the chains were attached to the silicate layers when CTA-1 was used. This low value is also in contrast to the 20% found in the analogous styrene polymerization, and correlates well with the fact that the PMMA-MMT-VB16 sample was poorly dispersed (see below) relative to the PS-MMT-VB16. It seems that with little dispersion of the silicate layers, most of the VB16 groups are unavailable to partake in the polymerization. Thus swelling, and preferably exfoliation, of the silicate layers by monomer is important in including the polymerizable surfactant in the polymerization process.

XRD patterns of the samples taken from the kinetic

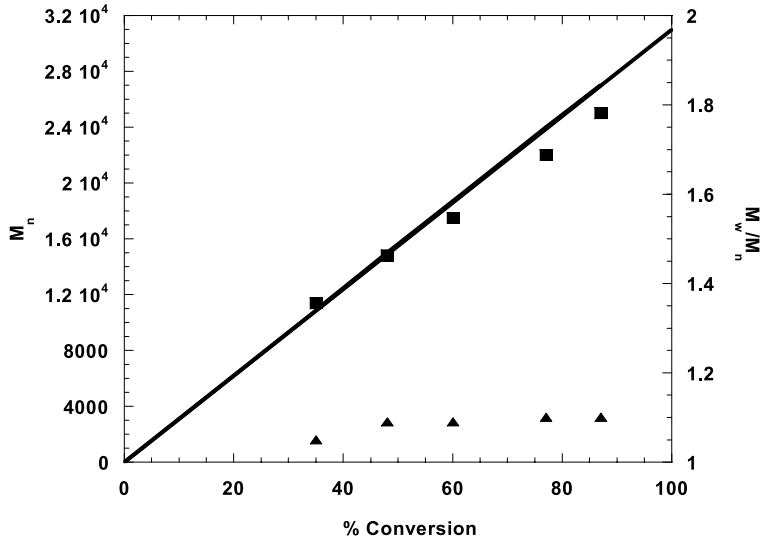

Fig. 3. Evolution of M_n (■) and (▲) M_w/M_n of PS extracted from PS-MMT-VB16 samples measured by GPC with the monomer conversion. (—) theoretical M_n.

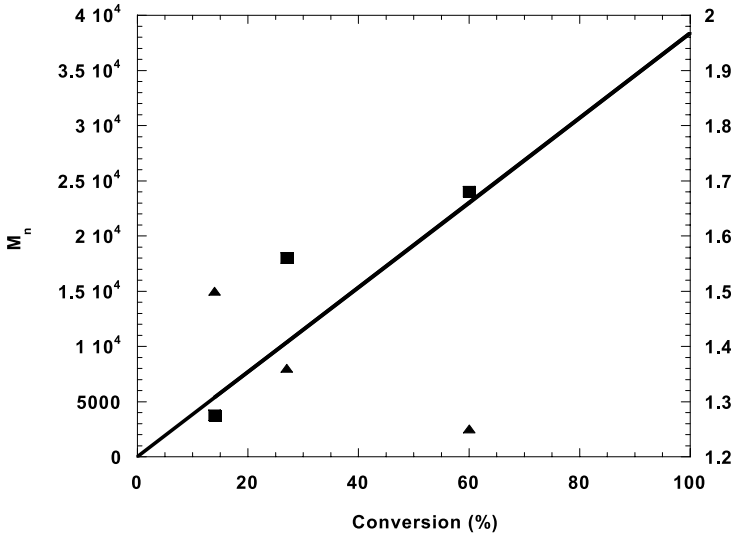

Fig. 4. Evolution of M_n (■) and (▲) M_w/M_n of PBA extracted from PBA-MMT-VB16 samples measured by GPC with the monomer conversion. (—) theoretical M_n.

experiments were also determined. These are shown in Figs. 7–9. For the PS sample the XRD data show that the silicate structure is lost within 5 h of the start of the reaction since the peak in the XRD pattern had disappeared by this time. This may indicate that the sample is exfoliated, although TEM is needed to confirm this (see below). To examine the dispersion of the MMT-VB16 in styrene further, we added approximately 40 wt% MMT-VB16 to styrene (with no initiator or CTA) and heated at 80 °C for 3 h. The slurry was then studied by XRD. There was no peak in the XRD spectrum (it was similar to the final sample in Fig. 7). The choice of 40 wt% MMT-VB16 in styrene was dictated by the experimental XRD set-up. It was reasoned that if 40 wt% MMT-VB16 in styrene exfoliated, then the lower 3% MMT-VB16 to styrene would also be exfoliated. Styrene itself was heated at 80 °C for 3 h then analyzed by GPC for the presence of polymer. It was found that only conversion was only 2% and $M_n = 860{,}000$. This indicates that styrene by itself is able to significantly disperse the silicate layers, and that polymer may not be required.

The XRD data for the PBA nanocomposite (Fig. 8) is similar to that of the PS nanocomposite. The silicate layers in the nanocomposite material seem to be significantly disordered by around 10 h. The peaks present in the XRD patterns of the samples taken at early times show that the silicate layers swell, moving apart and eventually becoming significantly dispersed at around 10 h into the reaction. Overtones of the first peak also appear within the early time spectra. A mixture of BA and ~40 wt% MMT-VB16 containing no initiator or CTA was heated at 60 °C for 3 h

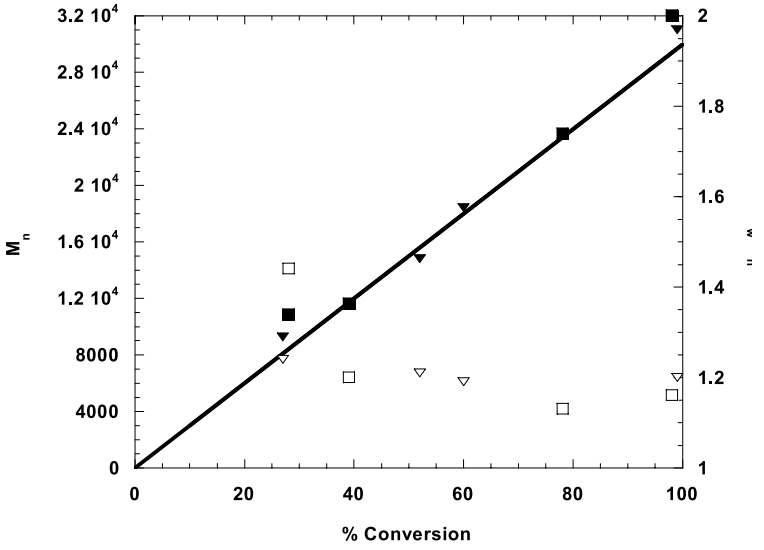

Fig. 5. Evolution of M_n (■, ▼) and (□, ▽) M_w/M_n of PMMA extracted from PMMA-MMT-VB16 samples, measured by GPC, prepared using CTA-1 and CTA-2, respectively, with the monomer conversion. (—) theoretical M_n.

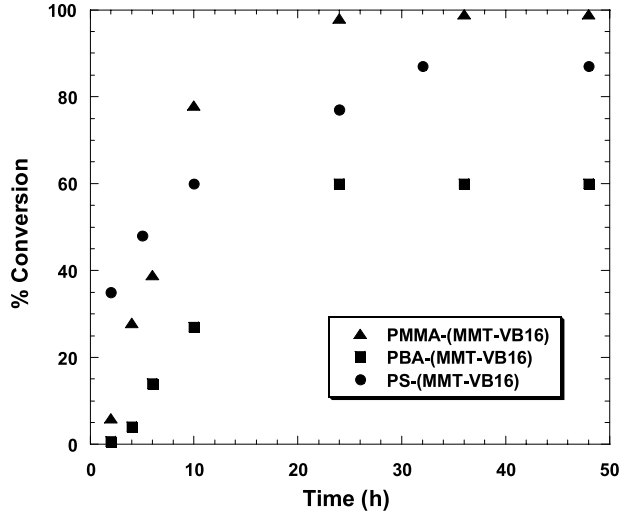

Fig. 6. Kinetic plots of PBA-MMT-VB16, PMMA-MMT-VB16 (using CTA-1), and PS-MMT-VB16 RAFT polymerizations.

together and analyzed with XRD. The XRD pattern showed a peak at ~2.5°, indicating that BA itself is unable to disperse the clay platelets, in contrast to the styrene case. Here, it appears that it is necessary to have polymer present in order to achieve exfoliation.

The XRD patterns for the PMMA nanocomposite, however, evolve quite differently to those of the PS and PBA materials. As Fig. 9 shows, there is still silicate structure at 10 h, which corresponds to 98% monomer conversion. The peak at the lowest angle in the XRD spectra hardly moves during the reaction (overtones are also present). This indicates that the final morphology of the PMMA-MMT-VB16 nanocomposite is not exfoliated, but may be a mixture of either unmixed, intercalation or exfoliated. Mixing MMA with the MMT-VB16 without initiator or CTA for up to 24 h at 60 °C did not give a fully dispersed system, as there was a peak at ~2.0° in the XRD spectrum. Therefore, for MMA neither the monomer nor the polymer facilitates exfoliation under the

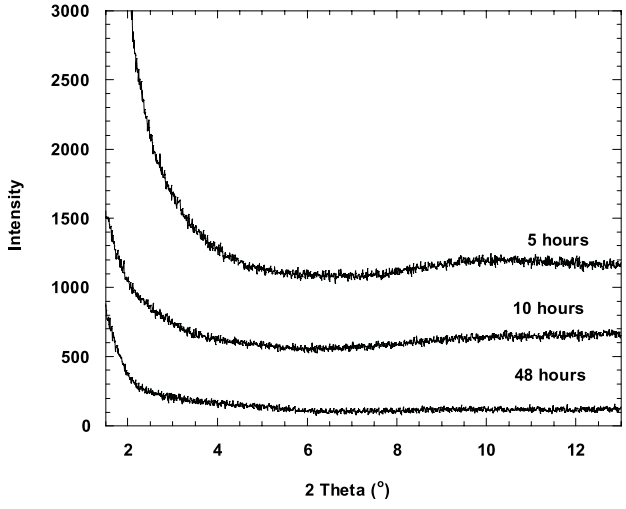

Fig. 7. XRD pattern of PS-MMT-VB16.

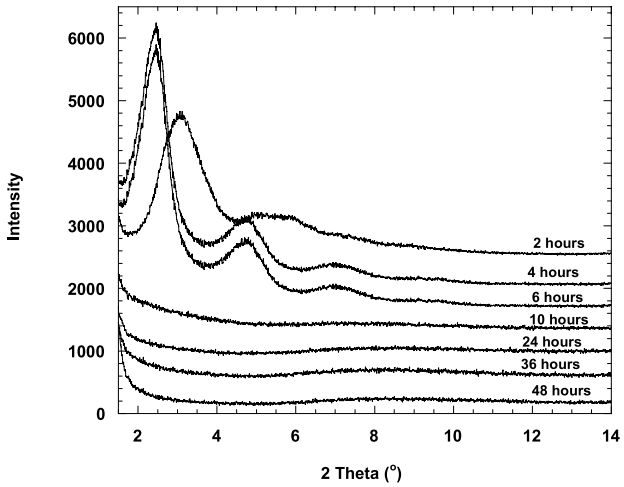

Fig. 8. XRD pattern of PBA-MMT-VB16.

conditions used in this study; this appears to be due to unfavorable mixing between the monomer and VB16.

To further examine the morphology development during the polymerization TEM was used. The TEM image (Fig. 10) of PS-MMT-VB16 sample (48 h) confirmed the presence of the exfoliated structure and the good dispersion of the silicate layers in the polymer matrix. On the other hand, the TEM image of PMMA-MMT-VB16 (Fig. 11) confirmed the XRD results in term of showing a significant degree of intercalation between the silicate layers in the polymer matrix. Similar results have been obtained by Wilkie et al. [15] when using MMT-VB16 to prepare PS and PMMA nanocomposite using conventional polymerization. TEM analysis was unable to be performed on the low T_g PBA nanocomposite sample, but based on the similarities of the XRD results of the PS and PBA nanocomposites we presume that the PBA sample was exfoliated.

In order to get an exfoliated PMMA nanocomposite MMT was modified with MA16, which was subsequently used to prepare PMMA nanocomposites. The primary

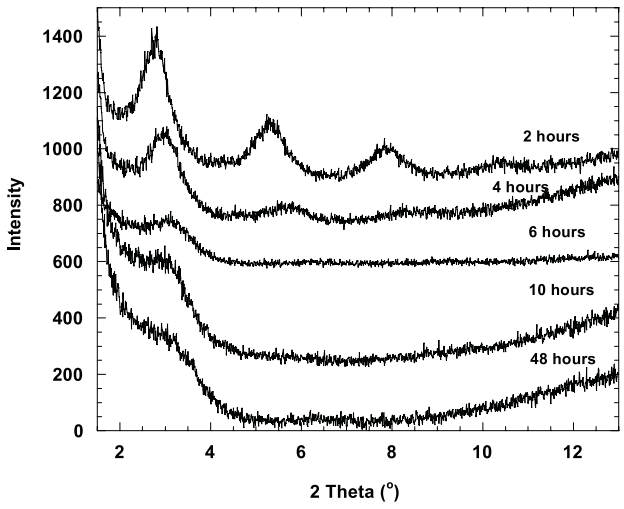

Fig. 9. XRD pattern of PMMA-MMT-VB16.

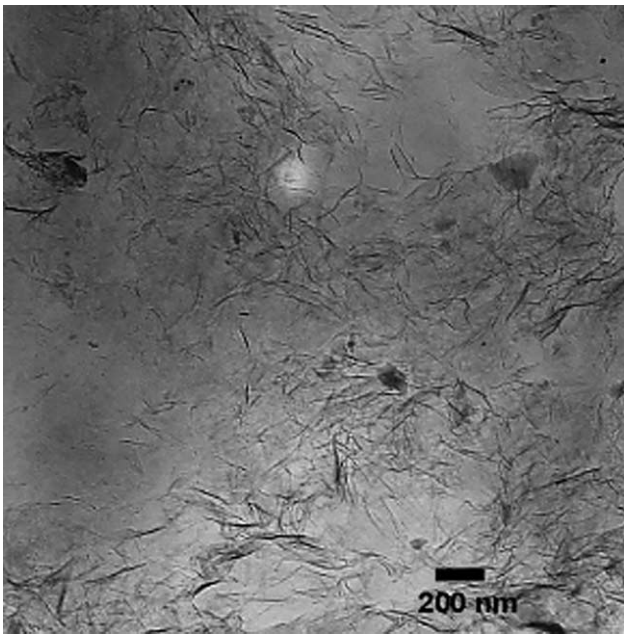

Fig. 10. TEM of PS-MMT-VB16 for the sample taken after 48 h, M_n= 25,000 and clay content of 3 wt%.

difference between this system and the VB16-based materials is that MA16 has a methacrylate polymerizable group instead of styryl group in VB16, which could result in better mixing with MMA or PMMA. Zeng and Lee [5] used MA16 modified clay to prepare PMMA nanocomposite using conventional radical polymerization. They found that the nanocomposite had an exfoliated structure, which agrees with our results as shown in the XRD spectrum (Fig. 12). The molecular weight of the produced polymer was 33,000 g/mol and the polydispersity was 1.24. The fact that MA16 leads to exfoliation, whereas VB16 does not, demonstrates the fact that the choice of organic modifier is very important when determining conditions for exfoliation. In particular, it appears that matching the structure, and

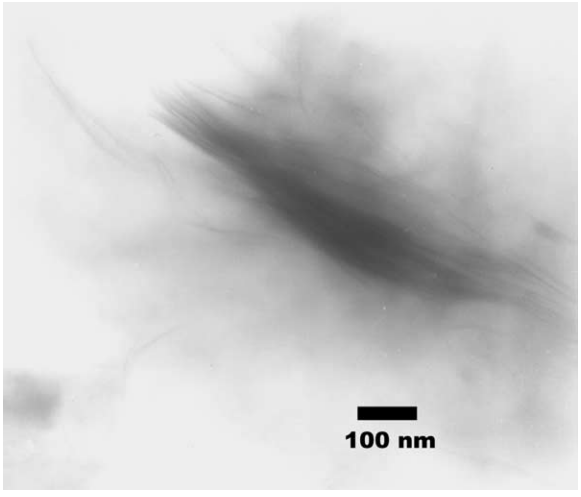

Fig. 11. TEM of PMMA-MMT-VB16 for the sample taken after 48 h, M_n= 32,000 and clay content of 3 wt%.

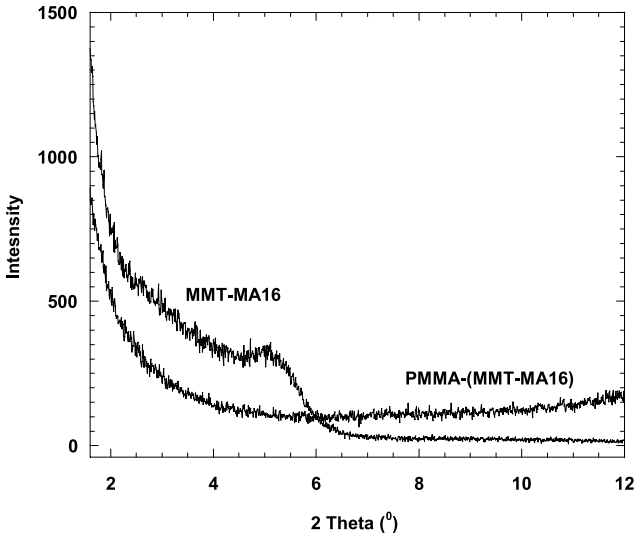

Fig. 12. XRD pattern of PMMA-MMT-MA16, and MMT-MA16.

thereby polarity, reactivity, etc. of the surfactant with the monomer enhances silicate dispersion. Furthermore, it appears that RAFT polymerizations provide the same morphologies as do conventional radical polymerizations for the VB16- and MA16-based nanocomposites.

We have also examined the thermal properties of the nanocomposites through TGA. The TGA of the nanocomposites and the corresponding free polymer (no clay present) were obtained for the final sample (the 48 h reaction time samples). As an example, shown in Fig. 13 are the TGA plots for the PS and PS-MMT sample. The TGA data for all samples is summarized in Table 1. These data indicate that the nanocomposite has better thermal stability than the free polymer based on the difference in the temperature at which the polymer nanocomposite and the free polymer loses 50% of the weight. In each case this was about 20–40 °C. The TGA results also provide an indication of the amount of

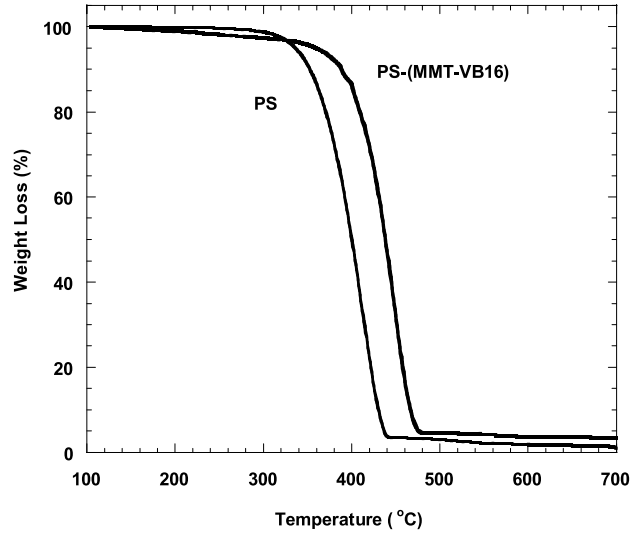

Fig. 13. TGA of PS and PS-MMT-VB16 nanocomposite.

Table 1
The temperature of 50% weight loss of both the polymer and polymer nanocomposite of PS, PBA, and PMMA

Sample	Temperature of 50% weight loss
PS	399
PS-(MMT-VB16)	437
PBA	416
PBA-(MMT-VB16)	438
PMMA	382
PMMA-(MMT-VB16)	401
PMMA-(MMT-MA16)	402

silicate in the nanocomposites. In the PS nanocomposite there is 3.0 wt% of clay in the polymer which is in reasonably good agreement with the expected value (2.6 wt%) calculated on the basis of the amount of the starting materials and the monomer conversion (83.0%). Similar results were obtained for both the PBA and PMMA nanocomposites. For the PBA nanocomposite, the actual contents of clay was found to be 4.17% compared to theoretical value of 3.7%, while for PMMA nanocomposite the actual clay content was found to be 2.4% compared to theoretical value of 2.2%.

4. Conclusions

RAFT polymerization in the presence of organically modified clay was shown to be successful techniques in preparing PS-, PMMA-, and PBA-layered silicate nanocomposites. The polymers had well-defined molecular weights and low polydispersities. The morphology of PS-, and PBA-nanocomposites were found to be exfoliated using MMT-VB16. In the case of PMMA nanocomposite, the structure was a mixture of unmixed/intercalated and exfoliated when MMT-VB16 was used, while the use of MMT-MA16 resulted in exfoliation. Previous work on these same MMT-based nanocomposites with conventional radical polymerizations gave similar results in terms of morphologies, and so it appears that RAFT polymerization does not result in significant differences in the morphologies obtained. These results clearly indicate that RAFT polymerization has the potential to synthesize a wide variety of exfoliated PLSNs based on the common styrene and (meth)acrylate families of monomers. As such, many combinations of these monomers and the construction of novel polymer architectures can be achieved using the methods presented here.

Acknowledgements

The following bodies are gratefully acknowledged for their financial support: Kuraray America, Inc., the Center for Advanced Materials Processing at Clarkson University (a New York State Center for Advanced Technology), and the Donors of The Petroleum Research Fund, administered by the American Chemical Society. Stacey Reeder and Mahesh Thopasridharan are thanked for helpful discussions and technical assistance, as is Prof T. Budd (St Lawrence University) for help with the ultramicrotome.

References

[1] Alexandre M, Dubois P. Mater Sci Eng 2000;R28:1.
[2] Messersmith PB, Giannelis EP. J Polym Sci, Part A: Polym Chem 1995;33:1047.
[3] Pinnavaia TJ, Beall GW, editors. Polymer–clay nanocomposites. New York: Wiley; 2000.
[4] Zanetti M, Lomakin S, Camino G. Macromol Mater Eng 2000;279:1.
[5] Zeng C, Lee LJ. Macromolecules 2001;34:4098.
[6] Burnside SD, Giannelis EP. J Polym Sci, Part B: Polym Phys 2000;38:1595.
[7] Giannelis EP, Krishnamoorti R, Manias E. Adv Polym Sci 1999;138:107.
[8] Krishnamoorti R, Giannelis EP. Macromolecules 1997;30:4097.
[9] Krishnamoorti R, Silva AS. Rheological properties of polymer layered-silicate nanocomposites. In: Pinnavaia TJ, Beall GW, editors. Polymer–clay nanocomposites. New York: Wiley; 2000. p. 315.
[10] Su S, Wilkie CA. J Polym Sci, Part A: Polym Chem 2003;41:1124.
[11] Zhu J, Morgan AB, Lamelas FJ, Wilkie CA. Chem Mater 2001;13:3774.
[12] Suprakas SR, Masami O. Prog Polym Sci 2003;28:1539.
[13] Kojima Y, Usuki A, Kawasumi M, Okada A, Fukushima Y, Kurauchi T, et al. J Mater Res 1993;8:1185.
[14] Zhao H, Shipp DA. Chem Mater 2003;15:2693.
[15] Zhao H, Argoti SD, Farrell BP, Shipp DA. J Polym Sci, Part A: Polym Chem 2004;41:916.
[16] Zhao H, Farrell BP, Shipp DA. Polymer 2004;45:4473.
[17] Böttcher H, Hallensleben ML, Nuss S, Wurm H, Bauer J, Behrens P. J Mater Chem 2002;12:1351.
[18] Weimer MW, Chen H, Giannelis EP, Sogah DY. J Am Chem Soc 1999;121:1615.
[19] Xu L, Reeder SR, Thopasridharan M, Ren J, Shipp DA, Krishnamoorti R. Nanotechnology, in press.
[20] Shipp DA. J Macromol Sci, Part C: Polym Rev 2005;45:171.
[21] Rizzardo E. Chem Aust 1987;54:32.
[22] Wang JS, Matyjaszewski K. J Am Chem Soc 1995;117:5614.
[23] Moad G, Solomon DH. The chemistry of free radical polymerization. Oxford: Pergamon; 1995.
[24] Hawker CJ. Trends Polym Sci 1996;4:183.
[25] Hawker CJ. Angew Chem, Int Ed 1995;34:1456.
[26] Puts RD, Sogah DY. Macromolecules 1996;29:3323.
[27] Greszta D, Matyjaszewski K. Macromolecules 1996;29:7661.
[28] Xia J, Matyjaszewski K. Macromolecules 1997;30:7697.
[29] Benoit D, Grimaldi S, Finet JP, Tordo P, Fontanille M, Gnanou Y. Controlled/living free-radical polymerization of styrene and *n*-butyl acrylate in the presence of a novel asymmetric nitroxyl radical. In: Matyjaszewski K, editor. Controlled radical polymerization. Washington, DC: American Chemical Society; 1998. p. 225.
[30] Betts DE, Johnson T, LeRoux D, DeSimone JM. Controlled radical polymerization methods for the synthesis of nonionic surfactants for CO_2. In: Matyjaszewski K, editor. Controlled radical polymerization. Washington, DC: ACS; 1998. p. 418.
[31] Chiefari J, Chong YKB, Ercole F, Krstina J, Jeffery J, Le TPT, et al. Macromolecules 1998;31:5559.
[32] Mitsukami Y, Donovan SM, Lowe AB, McCormick CL. Macromolecules 2001;34:2248.

[33] Thang SH, Rizzardo E, Moad G. Tetrahedron Lett 1999.
[34] Barner-Kowollik C, Quinn JF, Morsley DR, Davis TP. J Polym Sci, Part A: Polym Chem 2001;39:1353.
[35] Perrier S, Barner-Kowollik C, Quinn JF, Vana P, Davis TP. Macromolecules 2002;35:8300.
[36] Barners-Kowollik C, Coote ML, Davis TP, Radom L, Vana P. J Polym Sci, Part A: Polym Chem 2003;41:2828.
[37] Wang AR, Zhu SP, Kwak YW, Goto A, Fukuda T, Monteiro MS. J Polym Sci, Part A: Polym Chem 2003;41:2833.
[38] Kwak Y, Goto A, Fukuda T. Macromolecules 2004;37:1219.
[39] Kwak Y, Goto A, Komatsu K, Sugiura Y, Fukuda T. Macromolecules 2004;37:4434.
[40] Calitz FM, McLeary JB, McKenzie JM, Tonge MP, Klumperman B, Sanderson RD. Macromolecules 2003;36:9687.
[41] McLeary JB, Calitz FM, McKenzie JM, Tonge MP, Sanderson RD, Klumperman B. Macromolecules 2004;37:2383.
[42] McLeary JB, McKenzie JM, Tonge MP, Sanderson RD, Klumperman B. Chem Commun 2004;1950.